

Glycine N-Methyltransferase—/— Mice Develop Chronic Hepatitis and Glycogen Storage Disease in the Liver

Shih-Ping Liu,¹ Ying-Shiuan Li,¹ Yann-Jang Chen,² En-Pei Chiang,³ Anna Fen-Yau Li,⁴ Ying-Hue Lee,⁵ Ting-Fen Tsai,² Michael Hsiao,⁶ Shiu-Feng Hwang,⁷ and Yi-Ming Arthur Chen^{1,8}

Glycine N-methyltransferase (GNMT) affects genetic stability by regulating DNA methylation and interacting with environmental carcinogens. To establish a *Gnmt* knockout mouse model, 2 lambda phage clones containing a mouse *Gnmt* genome were isolated. At 11 weeks of age, the *Gnmt*—/— mice had hepatomegaly, hypermethioninemia, and significantly higher levels of both serum alanine aminotransferase and hepatic S-adenosylmethionine. Such phenotypes mimic patients with congenital GNMT deficiencies. A real-time polymerase chain reaction analysis of 10 genes in the one-carbon metabolism pathway revealed that 5,10-methylenetetrahydrofolate reductase, S-adenosylhomocysteine hydrolase (*Ahcy*), and formiminotransferase cyclodeaminase (*Ftcd*) were significantly down-regulated in *Gnmt*—/— mice. This report demonstrates that GNMT regulates the expression of both *Ftcd* and *Ahcy* genes. Results from pathological examinations indicated that 57.1% (8 of 14) of the *Gnmt*—/— mice had glycogen storage disease (GSD) in their livers. Focal necrosis was observed in male *Gnmt*—/— livers, whereas degenerative changes were found in the intermediate zones of female *Gnmt*—/— livers. In addition, hypoglycemia, increased serum cholesterol, and significantly lower numbers of white blood cells, neutrophils, and monocytes were observed in the *Gnmt*—/— mice. A real-time polymerase chain reaction analysis of genes involved in the gluconeogenesis pathways revealed that the following genes were significantly down-regulated in *Gnmt*—/— mice: fructose 1,6-bisphosphatase, phosphoenolpyruvate carboxykinase, and glucose-6-phosphate transporter. **Conclusion:** Because *Gnmt*—/— mice phenotypes mimic those of patients with GNMT deficiencies and share several characteristics with GSD Ib patients, we suggest that they are useful for studies of the pathogenesis of congenital GNMT deficiencies and the role of GNMT in GSD and liver tumorigenesis. (HEPATOLOGY 2007;46:1413-1425.)

Abbreviations: AGL, amylo-1,6-glucosidase; AHCY, S-adenosylhomocysteine hydrolase; ALDH1L1, aldehyde dehydrogenase 1 family member L1; ALT, alanine aminotransferase; AST, aspartate aminotransferase; ATIC, 5-aminoimidazole-4-carboxamide ribonucleotide formyltransferase/IMP cyclohydrolase; bp, base pair; CBS, cystathionine beta-synthase; FBPI, fructose 1,6-bisphosphatase; FISH, fluorescence in situ hybridization; FTCD, formiminotransferase cyclodeaminase; G6Pase, glucose-6-phosphatase; G6PT, glucose-6-phosphate transporter; GAA, α -glucosidase; GAPDH, glyceraldehyde 3-phosphate dehydrogenase; GBE1, branching enzyme 1; GNMT, glycine N-methyltransferase; GSD, glycogen storage disease; GYS2, glycogen synthase 2; HE, hematoxylin and eosin; kb, kilobase; mRNA, messenger RNA; MS, methionine synthase; MTHFR, 5,10-methylenetetrahydrofolate reductase; MTHFS, 5,10-methylenetetrahydrofolate synthetase; PAS, periodic acid-Schiff; PCR, polymerase chain reaction; PEPCK, phosphoenolpyruvate carboxykinase; PEX6, peroxisome biogenesis factor 6; PHKA2, phosphorylase kinase alpha 2; PYGL, glycogen phosphorylase; RT-PCR, reverse-transcription polymerase chain reaction; SAH, S-adenosylhomocysteine; SAM, S-adenosylmethionine; SHMT2, serine hydroxymethyl transferase 2; WT, wild-type.

From the ¹Division of Preventive Medicine, Institute of Public Health, School of Medicine, and ²Faculty of Life Sciences and Institute of Genome Sciences, National Yang-Ming University, Taipei, Taiwan; ³Department of Food Science and Biotechnology, National Chung Hsing University, Taichung, Taiwan; ⁴Department of Pathology, Veterans General Hospital, Taipei, Taiwan; ⁵Institute of Molecular Biology and ⁶Genetics Research Center, Academia Sinica, Taipei, Taiwan; ⁷Division of Molecular and Genomic Medicine, National Health Research Institutes, Miaoli, Taiwan; and ⁸Department of Microbiology, School of Medicine, National Yang-Ming University, Taipei, Taiwan.

Received March 20, 2007; accepted June 6, 2007.

Supported in part by a grant from the National Research Program on Genomic Medicine of the National Science Council of the Republic of China (grant number NSC95-3112-B-010-010).

Address reprint requests to: Yi-Ming Arthur Chen, Department of Microbiology, National Yang-Ming University, Shih-Pai, Taipei 112, Taiwan. E-mail: arthur@ym.edu.tw; fax: 886-2-28270576.

Copyright © 2007 by the American Association for the Study of Liver Diseases.

Published online in Wiley InterScience (www.interscience.wiley.com).

DOI 10.1002/hep.21863

Potential conflict of interest: Nothing to report.

Supplementary material for this article can be found on the HEPATOLOGY Web site (<http://interscience.wiley.com/jpages/0270-9139/suppmat/index.html>).

Glycine N-methyltransferase (GNMT), also known as a 4S polycyclic aromatic hydrocarbon binding protein, has multiple functions. In addition to acting as a major folate binding protein,¹ it also regulates the ratio of S-adenosylmethionine (SAM) to S-adenosylhomocysteine (SAH) by catalyzing sarcosine synthesized from glycine.² We previously reported that *GNMT* is down-regulated in hepatocellular carcinoma.^{3,4} Results from a genetic epidemiological study indicate that *Gnmt* is a tumor susceptibility gene for liver cancer.⁵ In addition, we reported that GNMT binds benzo(a)pyrene and prevents DNA-adduct formation.⁶

In mice, GNMT expression is regulated by growth hormone, with the hepatocytes of female mice having up to 8 times the expression level normally found in male mice.⁷ There have been three reports of pediatric patients (2 boys and 1 girl) with congenital *GNMT* deficiencies resulting from a missense mutation in the *GNMT* gene.^{8,9} All 3 children had hypermethioninemia, clinical symptoms mimicking chronic hepatitis,^{8,9} and mild elevations of serum alanine aminotransferase (ALT) and aspartate aminotransferase (AST). The livers of an Italian girl and her older brother had hepatomegaly at 4.7 and 9.7 years of age, respectively; the Gypsy boy had no hepatomegaly at 5 years.^{8,9} The girl had stunted growth and suffered from emotional instability. Although SAM levels in the plasma of all 3 children increased, no or very little elevation in the SAH and homocysteine levels was observed.^{8,9} Liver biopsies showed mild centrilobular fibrosis and some eosinophils in the girl patient and mild hydropic degeneration in the Gypsy boy.^{8,9} This background triggered our decision to generate a *Gnmt* knockout mouse model to study the role of GNMT in liver physiology.

For this study, we isolated 2 lambda phage clones containing the mouse *Gnmt* gene. Fluorescence in situ hybridization (FISH) was used to identify the chromosomal location. We developed a *Gnmt* knockout mouse model and characterized the phenotypes of both male and female homozygous knockout (*Gnmt*^{-/-}) mice. The liver GNMT, SAM, SAH, serum homocysteine, and ALT concentrations were measured, and the genes involved in one-carbon metabolism pathways were analyzed. Because more than half of the *Gnmt*^{-/-} mice had abnormal glycogen accumulations in their livers, we also studied the expression levels of a panel of genes involved in glycogen metabolism. Those results indicated that several genes involved in either the one-carbon or glycogen metabolism pathway were down-regulated in *Gnmt*^{-/-} mice, thus suggesting a novel gene regulation mechanism via GNMT.

Materials and Methods

Mouse *Gnmt* Isolation and Characterization. A C57BL/6-strain mouse placental genomic DNA library constructed in lambda phage FIX II (Stratagene, La Jolla, CA) was used to isolate *Gnmt* genomic clones. Human *GNMT* complementary DNA was used as a probe; hybridization procedures were performed according to standard protocols described previously.¹⁰ Phage clones 3-2 (Fig. 1A) and 5-3, containing *Gnmt*, were sequenced with a shotgun DNA sequencing procedure according to standard protocols.¹¹ Phage clone 3-2 was digested with the NotI restriction enzyme and subcloned into pBluescript II KS (Stratagene) to generate plasmid pSK-3-2.

Chromosomal Localization. The FISH analysis was performed according to steps described previously¹² (for additional information, see the supplementary material).

Animal Experimentation. All mice were kept in a 12-hour light-dark-cycle room with water and standard mouse pellet chow. Liver lobes were separated and divided into 2 parts: 1 part was fixed in buffered formalin to perform hematoxylin and eosin (HE) stain and periodic acid-Schiff (PAS) stain pathological examinations, and the other was stored in liquid nitrogen for DNA, RNA, and protein analyses. All animal protocols were approved by the Institutional Animal Care and Use Committee of National Yang-Ming University.

Messenger RNA (mRNA) Isolation and Reverse-Transcription Polymerase Chain Reaction (RT-PCR). Samples from wild-type mice were obtained from whole embryos (7.5 and 9.5 days old), embryonic livers (12.5 and 13.5 days old), and the livers, kidneys, and brains of newborn mice. The methods of the RNA extraction and polymerase chain reaction (PCR) conditions are detailed in the supplementary material. The primer sequences are listed in Table 1.

Generating *Gnmt* Knockout Mice. A targeting vector was constructed and used to generate the *Gnmt* knockout mouse model. The methods are detailed in the supplementary material. At 4 weeks, 11 weeks, and 9 months of age, at least 3 mice in each group were sacrificed for different analyses. All the mice had been fasting for at least 8 hours before they were sacrificed.

Real-Time PCR for Determining the Genes Expression Profile. The primer sequences are listed in Table 1. Real-time PCR was used to determine the gene expression levels of the following: *Gnmt*; S-adenosylhomocysteine hydrolase (*Ahcy*); methionine synthase (*Ms*); cystathionine beta-synthase (*Cbs*); 5,10-methylenetetrahydrofolate reductase (*Mthfr*); methylenetetrahydrofolate dehydrogenase (oxidized nicotinamide adenine dinucleotide phosphate-dependent), methylenetetrahydrofolate

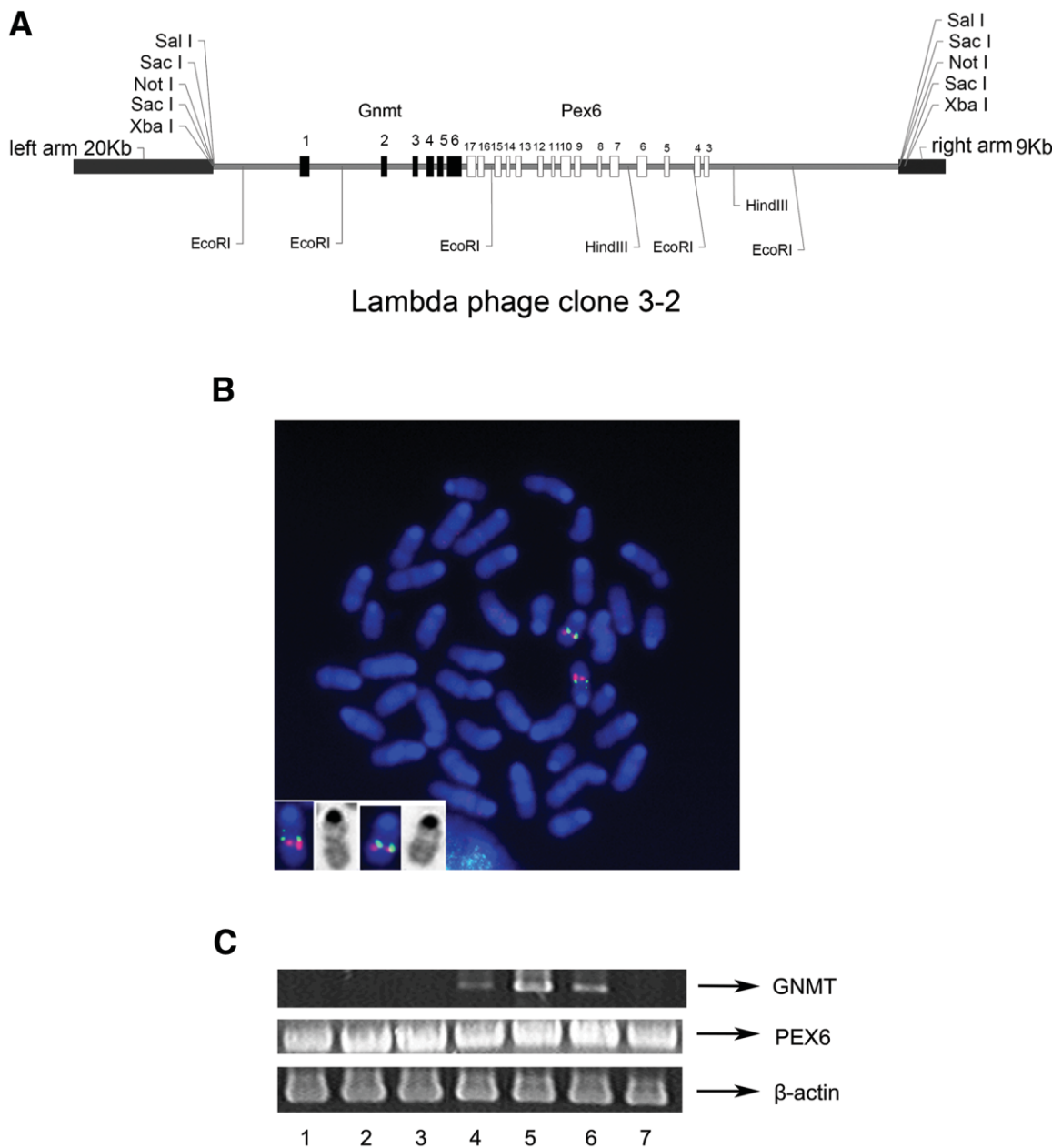


Fig. 1. Gene structure, localization, and expression profiles of mouse *Gnmt* and *Pex6* genes. (A) Lambda phage clone 3-2 containing the mouse *Gnmt* gene and exons 3-17 of the *Pex6* gene. Mouse *Gnmt* and *Pex6* nucleotide sequences have been deposited in GenBank with the respective accession numbers AY054408 and AY054409. (B) Representative metaphase following *in situ* hybridization with a probe containing partial *Gnmt* and *Pex6* genes. The metaphase was cohybridized with a mouse chromosome 17E probe (mouse PAC clone 669117) labeled with digoxigenin. The green fluorescents indicate specific *Gnmt/Pex6* hybridization signals detected by avidin-fluorescein isothiocyanate; the red fluorescents indicate the mouse chromosome 17E probe detected by the anti-digoxigenin antibody conjugated with rhodamine. (C) *Gnmt* and *Pex6* gene expression profiles in mouse embryos (lanes 1-4) and various organs of newborn mice (lanes 5-7): (1) a 7.5-day whole embryo, (2) a 9.5-day whole embryo, (3) a 12.5-day embryo liver, (4) a 13.5-day embryo liver, (5) a newborn mouse liver, (6) a newborn mouse kidney, and (7) a newborn mouse brain. Messenger RNA signals were detected with a reverse-transcription polymerase chain reaction. *Gnmt* indicates glycine N-methyltransferase; and *Pex6*, peroxisome biogenesis factor 6.

cyclohydrolase, formyltetrahydrofolate synthase (*Mthfd1*); aldehyde dehydrogenase 1 family member L1 (*Aldh1l1*); 5-aminoimidazole-4-carboxamide ribonucleotide formyltransferase/IMP cyclohydrolase (*Atic*); serine hydroxymethyltransferase 2 (*Shmt2*); 5,10-methylenetetrahydrofolate synthetase (*Mthfs*); formiminotransferase cyclodeaminase

(*Ftcd*); glycogen synthase 2 (*Gys2*); glucose-6-phosphatase (*G6Pase*); glucose-6-phosphate transporter (*G6PT*); α -glucosidase (*Gaa*); amylo-1,6-glucosidase (*AgI*); branching enzyme 1 (*Gbe1*); glycogen phosphorylase (*Ppyl*); phosphorylase kinase alpha 2 (*Phka2*); fructose 1,6-bisphosphatase (*Fbp1*); and phosphoenolpyruvate carboxykinase (*PEPCK*).

Table 1. Sequences of the Primers

Gene	Forward Primer	Reverse Primer
<i>Pex6</i>	GAGTGAGGACCGGGCTCCAGCT	CGCAACAGCTCCTGCTCACTGACTG
<i>Gnmt</i>	CGGGCGCCGCATGCTGGTGAAGAGGGC	GCGCTCGAGTCAGTCTGTCTCTTGAGCAC
<i>β-Actin</i>	GTGGGGCGCCCCAGGCACCA	CTCCTAATGTCACGCACGATTC
<i>Gnmt*</i>	CGGGCGCCGCATGCTGGTGAAGAGGGC	TGCACTGCGCAAGTGAGC
<i>Neomycin</i>	GTTCCTTGGCGCAGCTGTGCT	CGGCCACAGTCGATGAATCC
<i>Q-Gnmt</i>	GCCTACGTTCCCTGCTACTT	GCATTTGGGTGCAGATGTGG
<i>Ahcy</i>	GAAGGGTGCTCGCATTGCT	CCCAGGGCCACGAGAT
<i>Ms</i>	TTGAAAAATGTACAACAGCCTATGTC	TTTCATCATAGTCGCCAAAAGTGT
<i>Cbs</i>	GCTGAACCCAGACGGAGC	CCAGGACTGTCGGGATG
<i>Mthfr</i>	CTGCGGGTCAACTACCAC	CCACGTCACGGCATTGG
<i>Mthfd1</i>	CCAGAGGTGATCTAAATGACTGC	ACCCCTGCCTTTTGATGAG
<i>Aldh111</i>	TTCATAGGGCGGAGTTTG	CCATCCGTTGGGTTTATGTT
<i>Atic</i>	GCCCAAACCTCCCATCACAG	AGGCGTTCAAAGCGTCACA
<i>Shmt2</i>	CTGACCGCTCGGCTTTTC	AGTCAATGAGGCGGGCATAG
<i>Mthfs</i>	CACTGGTGGACTTGACCTC	CCAGCCGGTTGCCATC
<i>Ftcd</i>	GAAGCCCGAAAGGAGTGAAGA	GGGCCACTTAAGATAGTAAGGAATACT
<i>Gys2</i>	GGACTGGGCTGATCCTTTTCTC	GCAGTGTGGCATGGGTTGTA
<i>G6Pase</i>	TGGGCAAAATGGCAAGGA	ATTTCTGCCCCAGGAATCAA
<i>G6PT</i>	TGTGGAGCCAGCACAGTTGT	TGGATACTCGGCCCATCTTG
<i>Gaa</i>	CTTCAAGATCAAAGATCCTGCTAGTAAAG	TGAGAATCCACGCTGTAAGTGT
<i>AgI</i>	GGCATCACCGGCAGATACA	GGAGCCTATTGATGCCACATC
<i>Gbe1</i>	GCGATCATGGAACATGCTTACTAT	CCATAACGACTTGAAGCTGCAA
<i>Pygl</i>	CATGGGCGCAACATTACAGAA	CCAATCCAAGCTGGTAAATGG
<i>Phka2</i>	AGAAGCACCTGGGATCATTTT	GTTCTTTTGGAGTCCATGAGA
<i>Fbp1</i>	ATGAGGGTTATGCCAAGCACTTT	CCATCCGAGGGAACCTTTT
<i>PEPCK</i>	GCTCCTGGCACCTCAGTGAA	ACGTTGGTGAAGATGGTGTTT
<i>GAPDH</i>	TGGTATCGTGAAGGACTCA	AGTGGGTGCTGCTGTGAAG

*Gnmt** primers were used for genotyping, *Gnmt* primers were used for RT-PCR analysis, and *Q-Gnmt* primers were used for real-time PCR. *AgI* indicates amylo-1,6-glucosidase; *Ahcy*, S-adenosylhomocysteine hydrolase; *Aldh111*, aldehyde dehydrogenase 1 family member L1; *Atic*, 5-aminoimidazole-4-carboxamide ribonucleotide formyltransferase/IMP cyclohydrolase; *Cbs*, cystathionine beta-synthase; *Fbp1*, fructose 1,6-bisphosphatase; *Ftcd*, formiminotransferase cyclodeaminase; *G6Pase*, glucose-6-phosphatase; *G6PT*, glucose-6-phosphate transporter; *Gaa*, α-glucosidase; *GAPDH*, glyceraldehyde 3-phosphate dehydrogenase; *Gbe1*, branching enzyme 1; *Gnmt*, glycine N-methyltransferase; *Gys2*, glycogen synthase 2; *Ms*, methionine synthase; *Mthfd1*, methylenetetrahydrofolate dehydrogenase (oxidized nicotinamide adenine dinucleotide phosphate-dependent) 1, methylenetetrahydrofolate cyclohydrolase, formyltetrahydrofolate synthase; *Mthfr*, 5,10-methylenetetrahydrofolate reductase; *Mthfs*, 5,10-methylenetetrahydrofolate synthetase; *PEPCK*, phosphoenolpyruvate carboxykinase; *Pex6*, peroxisome biogenesis factor 6; *Phka2*, phosphorylase kinase alpha 2; *Pygl*, glycogen phosphorylase; and *Shmt2*, serine hydroxymethyl transferase 2.

Complementary DNA was produced from hepatic RNA (5 μg). The procedures of real-time PCR analysis have been described.¹³

Determining the Blood Biochemical Parameters and Hematological Analysis in *Gnmt*^{-/-} Mice. The concentrations of plasma methionine were determined by tandem mass spectrometry. The serum homocysteine was measured with a high-performance liquid chromatograph equipped with fluorometric detection.¹⁴ The serum ALT and glucose were analyzed with a Fujifilm (Kanagawa, Japan) DRI-CHEM 3500s. The concentrations of the serum cholesterol, triglyceride, uric acid, urea, alkaline phosphatase, total protein, phosphorus, and creatinine were analyzed with an Abbott Alcyon 300i (Abbott Laboratories, Ltd., United States). The white blood cell, neutrophil, lymphocyte, monocyte, eosinophil, basophil, red blood cell, and platelet counts were analyzed with an Abbott Alcyon 3700 cell counter (Abbott Laboratories).

Results

Mouse *Gnmt* Gene Characterization. Two lambda phage clones (3-2 and 5-3, both containing mouse *Gnmt* genomic DNA) were isolated after the screening of more than 1×10^4 colonies from the mouse placental genomic DNA library with human *GNMT* complementary DNA as a probe. Shotgun DNA sequencing and a blast program were used to obtain full-length sequences [approximately 15 kilobases (kb)] of the 3-2 clone. Returns from a homology search using the Gene Blast program showed that *Gnmt* and exons 3-17 of the peroxisome biogenesis factor 6 (*Pex6*) gene were located on the left and right arms of clone 3-2, respectively (Fig. 1A). The *Gnmt* and *Pex6* genes were oriented tail to tail with a gap of 124 base pairs (bp) at their 3' ends.

Chromosomal *Gnmt* Gene Localization. The chromosomal localization of the mouse *Gnmt* gene was determined by FISH. Mouse metaphase chromosomes were cohybridized with a plasmid (pSK-3-2) DNA probe containing the *Gnmt* and a chromosome 17E probe

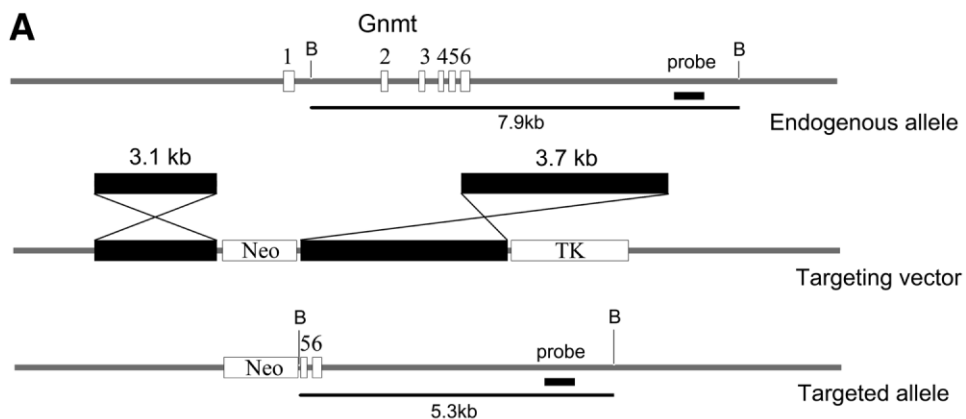
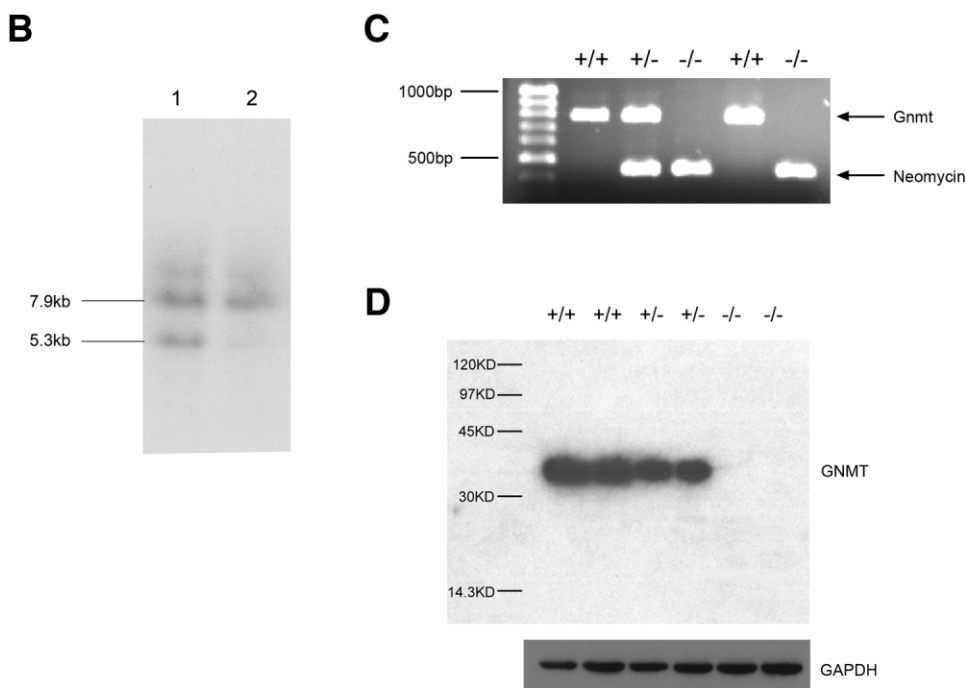


Fig. 2. Targeted modification of the *Gnmt* gene locus. (A) The targeting vector was designed to replace *Gnmt* exons 1-4 and part of exon 5 with a neomycin-resistance gene. The neomycin-positive selection marker is flanked by 2 homologous regions and followed by a thymidine kinase-negative selection marker at the 3' end of the targeting vector. (B) Southern blot analysis of embryonic stem cell clones. The BamHI (B)-BamHI DNA fragment size decreased from 7.9 (wild-type allele) to 5.3 kb (recombinant allele). (C) Genotyping of *Gnmt* knockout mice by a polymerase chain reaction. By the *Gnmt* and neomycin specific PCR, the normal *Gnmt* allele yielded a 772-bp fragment, and the disrupted allele yielded a 409-bp fragment. (D) Expression of the GNMT protein confirmed by a western blot analysis. Each lane contains 10 μ g of hepatic lysate. The GNMT molecular mass was 32 kDa, and GAPDH was used as an internal control. $-/-$ indicates *Gnmt* $-/-$ mice; $+/-$, *Gnmt* heterozygous mice; $+/+$, wild-type mice; GAPDH, glyceraldehyde 3-phosphate dehydrogenase; GNMT, glycine N-methyltransferase; and kb, kilobase.



(669I17). As shown in Fig. 1B, the mouse *Gnmt* gene was localized to chromosome 17C (green fluorescence).

***Gnmt* and *Pex6* Expression Profiles in Different Mouse Embryonic Stages and in Newborn Mouse Tissue.** We compared *Gnmt* and *Pex6* gene expression profiles at different embryonic stages and in organs of newborn mice. The RT-PCR results showed that *Pex6* transcripts could be detected in embryos as early as day 7.5 and that it was expressed throughout the embryonic development stages (Fig. 1C). Furthermore, *Pex6* was abundant in the livers, kidneys, and brains of newborn mice. In contrast, *Gnmt* transcripts were detected only during the last stage (day 13.5) of embryonic development (Fig. 1C, lane 4); these transcripts were found in the livers and kidneys of newborn mice but not in their brains.

Generating a *Gnmt* Knockout Mouse Model. A targeting vector (Fig. 2A) was constructed and used for transfer into embryonic stem cells via electroporation.

Cells containing recombinant genomes were differentiated with a Southern blot analysis. As shown in lane 1 of Fig. 2B, the size of the BamHI (B)-BamHI DNA fragment decreased from 7.9 (wild-type allele) to 5.3 kb (recombinant allele). The stem cell clone containing the recombinant allele was microinjected into blastocytes of C57BL/6 mice. We eventually obtained 4 male chimeric mice for germ-line transmission. PCR was developed to differentiate wild-type ($+/+$), *Gnmt* heterozygous ($+/-$), and *Gnmt* $-/-$ mice. The normal *Gnmt* allele yielded a 772-bp fragment by *Gnmt* primers, and the disrupted allele yielded a 409-bp fragment by neomycin primers (Fig. 2C). The expression of the GNMT protein in the liver was analyzed with a western blot (see the supplementary material); the results show that in comparison with the wild type, the GNMT expression decreased approximately 50% in the livers of *Gnmt* $+/-$ mice, and GNMT was undetectable in the livers of *Gnmt* $-/-$ mice (Fig. 2D).

Table 2. Concentrations of Hepatic SAM and SAH and Levels of Serum Homocysteine and Methionine from Wild-Type and *Gnmt* Knockout Mice

		SAM (nmol/g of liver)	SAH (nmol/g of liver)	SAM/SAH	Total Homocysteine (μ M)	Methionine (mg/dL)
Wild-type	Male	45.0 \pm 23.4	71.9 \pm 26.2	0.63	5.7 \pm 0.03	0.74 \pm 0.03
	Female	52.4 \pm 29.3	64.2 \pm 16.8	0.82	5.7 \pm 0.04	0.74 \pm 0.01
	Total	48.0 \pm 24.6	68.8 \pm 22.2	0.69	5.6 \pm 0.13	0.75 \pm 0.02
<i>Gnmt</i> ^{+/-}	Male	18.0 \pm 4.6	77.1 \pm 8.9	0.23	5.9 \pm 0.10	ND
	Female	16.2 \pm 10.2	70.4 \pm 11.9	0.23	5.9 \pm 0.20	ND
	Total	17.1 \pm 7.1	73.7 \pm 10.1	0.23	5.9 \pm 0.17	ND
<i>Gnmt</i> ^{-/-}	Male	3085.4 \pm 1276.9	73.3 \pm 33.6	42.09	5.8 \pm 0.10	2.04 \pm 0.64
	Female	3882.0 \pm 1978.8	57.7 \pm 6.2	67.28	5.8 \pm 0.30	2.47 \pm 0.89
	Total	3453.1 \pm 1617.9	66.5 \pm 25.4	51.93	5.8 \pm 0.19	2.23 \pm 0.76

ND indicates not determined; SAH, S-adenosylhomocysteine; and SAM, S-adenosylmethionine.

SAM and SAH Concentrations in the Livers of *Gnmt*^{-/-} Mice. At 11 weeks of age, male and female wild-type, *Gnmt*^{+/-}, and *Gnmt*^{-/-} mice (≥ 6 mice per group) were sacrificed for a phenotypic analysis. The SAM and SAH concentrations were detected with high-performance liquid chromatography (see the supplementary materials and methods). In comparison with wild-type mice of the same gender, the hepatic concentrations of SAM in *Gnmt*^{-/-} mice significantly increased in both male and female mice ($P < 0.05$). In contrast, the hepatic concentration of SAM in *Gnmt*^{+/-} mice was 2.8-fold lower than that in wild-type mice (Table 2), and the hepatic concentrations of SAH in male and female *Gnmt*^{-/-} mice were similar to those in the wild-type mice. Accordingly, the SAM/SAH ratio increased 42-fold and 82-fold in the male and female *Gnmt*^{-/-} mice, respectively (Table 2).

Serum Levels of Homocysteine and Methionine in *Gnmt*^{-/-} Mice. The homocysteine levels remained unchanged across the different mouse groups. The methionine levels in the *Gnmt*^{-/-} mice were 1.9-2.4-fold greater than those in the wild-type mice (Table 2).

Real-Time PCR Analysis of Genes Involved in the One-Carbon Metabolism Pathway. Real-time PCR analysis was used to analyze the mRNA levels in the following genes (involved in the one-carbon metabolism pathway) in both wild-type and *Gnmt*^{-/-} mice: *Gnmt*, *Ahcy*, *Ms*, *Cbs*, *Mthfr*, *Mthfd1*, *Aldh1l1*, *Atic*, *Shmt2*, *Mthfs*, and *Ftcd*. In comparison with the wild-type mice, the mRNAs of *Ahcy*, *Mthfr*, and *Ftcd* were significantly down-regulated in both male and female *Gnmt*^{-/-} mice ($P < 0.05$; Fig. 3). In terms of the gender difference in wild-type mice, the expression levels of *Gnmt*, *Cbs*, and *Mthfr* of male mice were significantly lower than those of female mice.

Liver Function of *Gnmt*^{-/-} Mice. The total body weights of the *Gnmt*^{-/-} and wild-type groups from the age of 1 week to the age of 9 months showed no significant

difference (data not shown). For mice sacrificed at 4 weeks, 11 weeks, and 9 months, the mean liver weight/total body weight ratios for the *Gnmt*^{-/-} mice were significantly higher than those for the wild-type mice, with 1 exception: 4-week-old male mice (Fig. 4A). This suggests hepatomegaly in the *Gnmt*^{-/-} mice, in the females prior to the males. In terms of *Gnmt*^{+/-} mice, the mean liver weight/total body weight ratios were slightly less than those of the wild-type mice at 11 weeks of age (Fig. 4A).

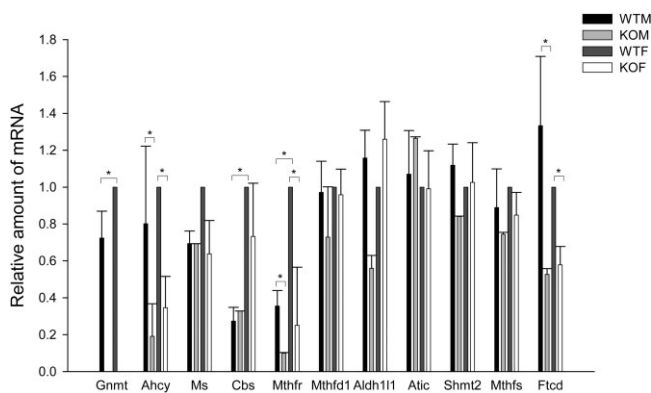


Fig. 3. Real-time polymerase chain reaction analyses of mRNA expression levels of the genes involved in the one-carbon metabolism pathway. The expression profiles of mRNA in WTM, KOM, and KOF liver tissue were normalized to the WTF mice. * $P < 0.05$. *Ahcy* indicates S-adenosylhomocysteine hydrolase; *Aldh1l1*, aldehyde dehydrogenase 1 family member L1; *Atic*, 5-aminoimidazole-4-carboxamide ribonucleotide formyltransferase/IMP cyclohydrolase; *Cbs*, cystathionine beta-synthase; *Ftcd*, formiminotransferase cyclodeaminase; *Gnmt*, glycine N-methyltransferase; KOF, *Gnmt*^{-/-} female; KOM, *Gnmt*^{-/-} male; mRNA, messenger RNA; *Ms*, methionine synthase; *Mthfd1*, methylenetetrahydrofolate dehydrogenase (oxidized nicotinamide adenine dinucleotide phosphate-dependent), methylenetetrahydrofolate cyclohydrolase, formyltetrahydrofolate synthase; *Mthfr*, 5,10-methylenetetrahydrofolate reductase; *Mthfs*, 5,10-methylenetetrahydrofolate synthetase; *Shmt2*, serine hydroxymethyl transferase 2; WTF, wild-type female; and WTM, wild-type male.

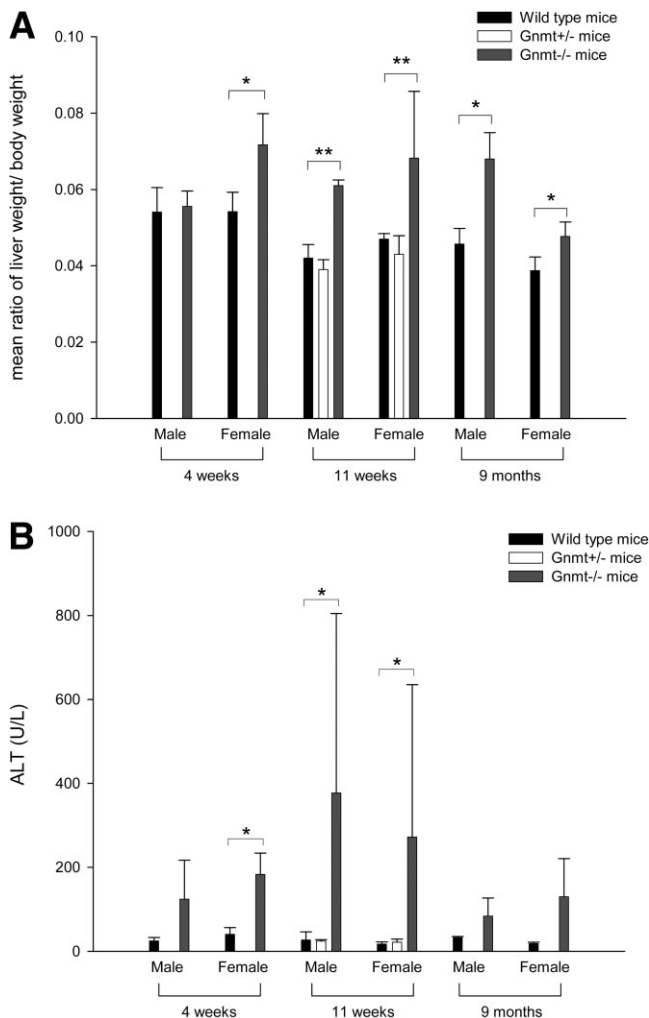


Fig. 4. *Gnmt*^{-/-} mice had hepatomegaly and significantly higher levels of serum ALT. (A) Ratio of the liver weight to the body weight. (B) Comparison of serum ALT levels between wild-type, *Gnmt*^{+/-}, and *Gnmt*^{-/-} mice. * $P < 0.05$ and ** $P < 0.01$ versus the wild-type mice. ALT indicates alanine aminotransferase; and *Gnmt*, glycine N-methyltransferase.

The results from serum ALT level measurements show that at the age of 4 weeks, the mean ALT level in the female *Gnmt*^{-/-} mice was significantly higher than that in the wild-type mice ($P < 0.05$), but there was no statistically significant difference between the male wild-type and *Gnmt*^{-/-} mice (Fig. 4B). At 11 weeks of age, the mean ALT levels of both male and female *Gnmt*^{-/-} mice were significantly higher than the levels of the wild-type mice ($P < 0.05$). At 9 months of age, the mean serum ALT levels were abnormal in both male and female *Gnmt*^{-/-} mice; the differences between the wild-type and *Gnmt*^{-/-} mice were not statistically significant (Fig. 4B).

Pathological Findings for *Gnmt*^{-/-} Mice. The overall appearances of the liver organs from both wild-type and *Gnmt*^{+/-} mice were relatively normal at the age

of 11 weeks (Fig. 5A,B), whereas male and female *Gnmt*^{-/-} mice of the same age had enlarged livers (Fig. 5C,D). Multiple gray-whitish nodules approximately 1 mm long were found in the livers of 6 of 7 male *Gnmt*^{-/-} mice (Fig. 5C). HE staining of histological mouse liver sections revealed no abnormalities in the *Gnmt*^{+/-} mice (Fig. 5F,J). However, we observed coagulative necrosis, sinusoidal dilatation, and congestion in the male *Gnmt*^{-/-} mice (Fig. 5G,K). Degenerative changes and perinuclear vacuoles were observed in the intermediate zones of livers in 5 of 7 female *Gnmt*^{-/-} mice (Fig. 5H,L).

PAS staining was used to examine glycogen storage in mouse liver tissue. In comparison with the male and female wild-type mice (Fig. 5M,N), abnormal storage patterns were found in 3 of 7 (42.9%) male and 5 of 7 (71.4%) female *Gnmt*^{-/-} mice (Fig. 5O,P). Glycogen accumulation was more severe in the female *Gnmt*^{-/-} mice. Glycogen was present in the cytoplasm and sinusoids of livers of female *Gnmt*^{-/-} mice (Fig. 5P) and in the cytoplasm but not the sinusoids of livers of male *Gnmt*^{-/-} mice (Fig. 5O). No pathological abnormalities were noted in the following organs of *Gnmt*^{-/-} mice: the heart, spleen, lungs, pancreas, stomach, kidneys, and small and large intestines. In addition, no abnormal glycogen storage was found in either the hearts or kidneys of the *Gnmt*^{-/-} mice (data not shown).

At the age of 9 months, HE staining of histological sections of mouse livers showed degenerative changes and perinuclear vacuoles in the intermediate zones of male and female *Gnmt*^{-/-} mice (Fig. 5Q,S). PAS staining showed that two-thirds of both male and female *Gnmt*^{-/-} mice had abnormal accumulations of glycogen in their livers (Fig. 5R,T).

Hematology and Analysis of the Blood Biochemical Parameters of *Gnmt*^{-/-} Mice. As shown in Fig. 6A, hematological examinations demonstrated that the *Gnmt*^{-/-} mice had significantly lower numbers of white blood cells, neutrophils, and monocytes than the wild-type mice ($n = 12$ for each group, $P < 0.05$). Although the *Gnmt*^{-/-} mice had lower numbers of lymphocytes, basophils, and eosinophils than the wild-type mice, the differences were not statistically significant ($P = 0.101$, 0.478 , and 0.078 , respectively; Fig. 6A). We also compared the following blood biochemical parameters between *Gnmt*^{-/-} and wild-type mice: the concentrations of serum glucose, cholesterol, triglyceride, uric acid, urea, alkaline phosphatase, total protein, phosphorus, and creatinine. The results showed that the *Gnmt*^{-/-} mice had significantly lower glucose levels ($P < 0.05$) and higher cholesterol levels ($P < 0.01$) than the wild-type mice (Fig. 6B). Although the serum triglyceride was lower in the

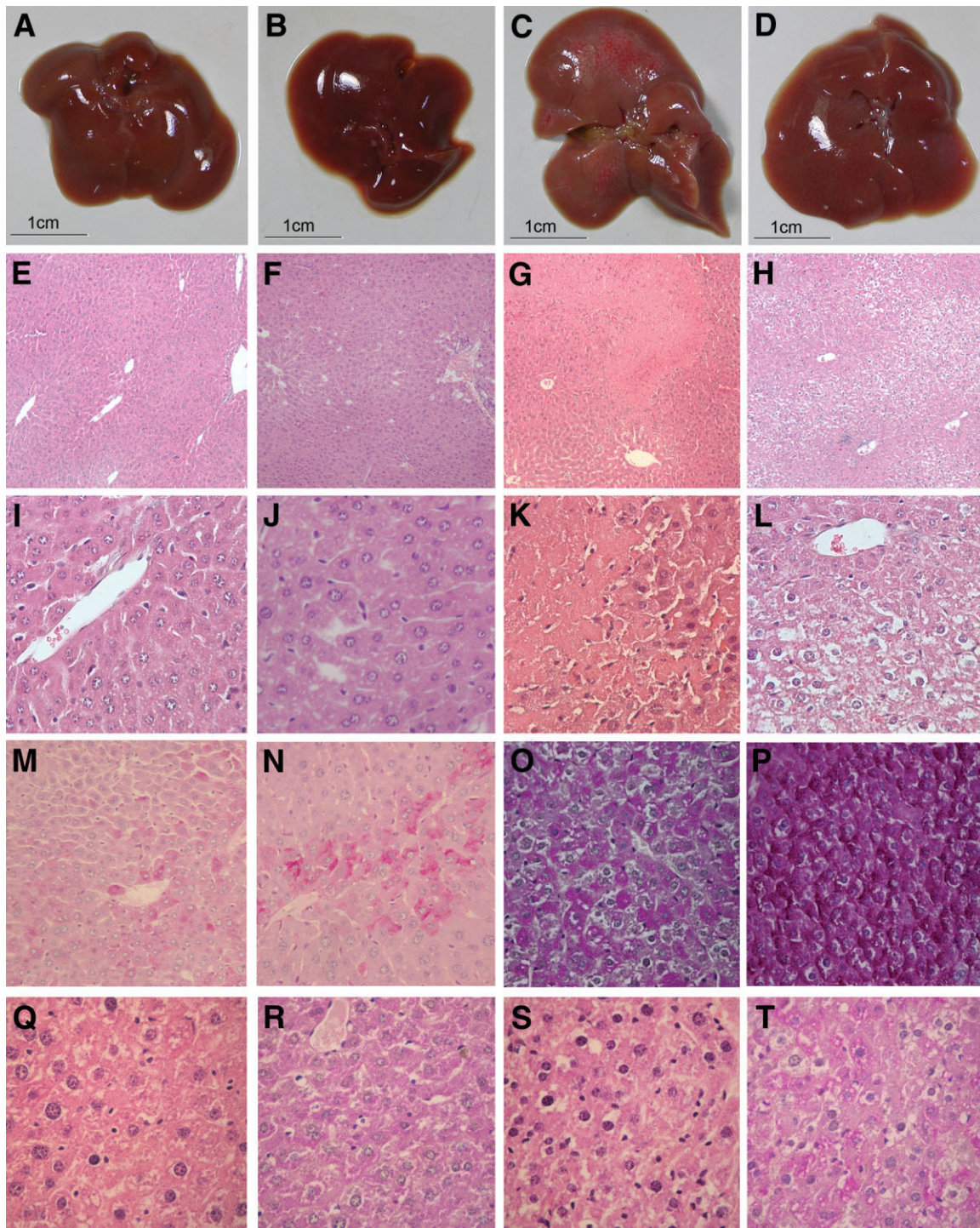


Fig. 5. Pathological examination of wild-type and *Gnmt*^{-/-} mouse livers. Gross pathology of liver organs from (A) 11-week-old male wild-type, (B) male *Gnmt*^{+/-}, (C) male *Gnmt*^{-/-}, and (D) female *Gnmt*^{-/-} mice. All the mice had been fasting for 8 hours before they were sacrificed. Hematoxylin and eosin staining of the liver tissue from (E,I) 11-week-old male wild-type, (F,J) male *Gnmt*^{+/-}, (G,K) male *Gnmt*^{-/-}, (H,L) female *Gnmt*^{-/-}, (Q) 9-month-old male *Gnmt*^{-/-}, and (S) 9-month-old female *Gnmt*^{-/-} mice. Periodic acid-Schiff staining of the liver tissue from (M) 11-week-old male wild-type, (N) female wild-type, (O) male *Gnmt*^{-/-}, (P) female *Gnmt*^{-/-}, (R) 9-month-old male *Gnmt*^{-/-}, and (T) 9-month-old female *Gnmt*^{-/-} mice. The magnification was (E-H) $\times 100$ or (I-T) $\times 400$. *Gnmt* indicates glycine N-methyltransferase.

Gnmt^{-/-} mice, the difference was not statistically significant. All levels of the other blood biochemical parameters in the *Gnmt*^{-/-} mice were within the normal range (data not shown).

Real-Time PCR Analysis of Genes Involved in Glycogen Metabolism. Results from a pathological examination revealed that *Gnmt*^{-/-} mice had abnormally high glycogen accumulations in their livers, so we used

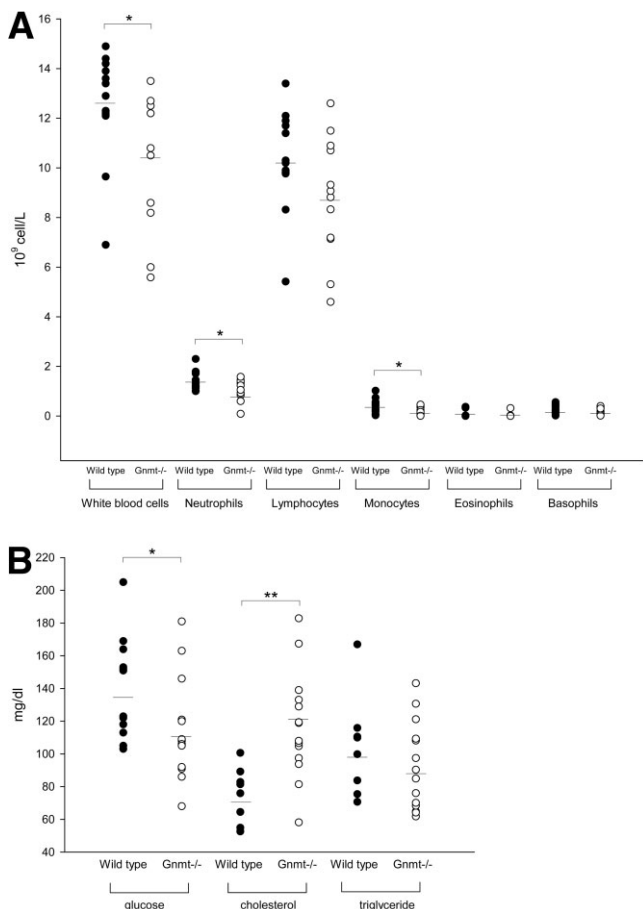


Fig. 6. Hematology and analysis of the blood biochemical parameters of wild-type and *Gnm1*^{-/-} mice. (A) White blood cell, neutrophil, lymphocyte, monocyte, eosinophil, and basophil counts of (●) wild-type mice and (○) *Gnm1*^{-/-} mice. The horizontal bars indicate the mean counts. (B) Serum glucose, cholesterol, and triglyceride levels of (●) wild-type mice and (○) *Gnm1*^{-/-} mice. The horizontal bars indicate the mean serum concentration. **P* < 0.05 and ***P* < 0.01 versus the wild-type mice. *Gnm1* indicates glycine N-methyltransferase.

real-time PCR to analyze the expression levels for genes linked with various types of glycogen storage disease (GSD): *Gys2*, *G6Pase*, *G6PT*, *Gaa*, *Ag1*, *Gbe1*, *Pygl*, and *Phka2*. In our analysis, we also included 2 rate-limiting enzymes involved in the gluconeogenesis pathway: *Fbp1* and *PEPCK*. As shown in Fig. 7A, the mRNA levels of the *G6PT*, *Gaa*, *Pygl*, and *PEPCK* genes in 14 *Gnm1*^{-/-} mice (7 male and 7 female) were significantly lower than those in 12 wild-type mice at 11 weeks of age. Next, we compared gene expression levels between 8 *Gnm1*^{-/-} mice (3 male and 5 female) with glycogen accumulations and 12 wild-type mice. The data indicate that all of the previously listed genes were expressed at much lower levels in glycogen-accumulated *Gnm1*^{-/-} mice (*P* < 0.01). In addition, the expression levels of *Gys2*, *Ag1*, *Gbe1*, and *Fbp1* in *Gnm1*^{-/-} mice with accumulated glycogen were also significantly lower (*P* < 0.05). We also noted that the

mRNA levels of *G6Pase*, *G6PT*, *Gaa*, *Pygl*, *Fbp1*, and *PEPCK* were lower in 9-month-old *Gnm1*^{-/-} mice; the differences between *Gnm1*^{-/-} and wild-type mice were not statistically significant (Fig. 7B).

Discussion

In this study, we used FISH to demonstrate that the mouse *Gnm1* gene is localized in the chromosome 17C region (Fig. 1B). This finding is consistent with data in the National Center for Biotechnology Information mouse genome project database (<http://www.ncbi.nlm.nih.gov/genome/guide/mouse/>). In addition, we found very different mRNA expression profiles of *Gnm1* and *Pex6* during various mouse embryonic stages and in the organs of newborn mice. *Pex6* transcripts were detected as early as day 7.5, whereas *Gnm1* transcripts were not detected until day 13.5. This suggests an absence of interaction between *Gnm1* and *Pex6* at the transcriptional level.

We measured hepatic SAM and SAH concentrations and found that the mean SAM concentration in the

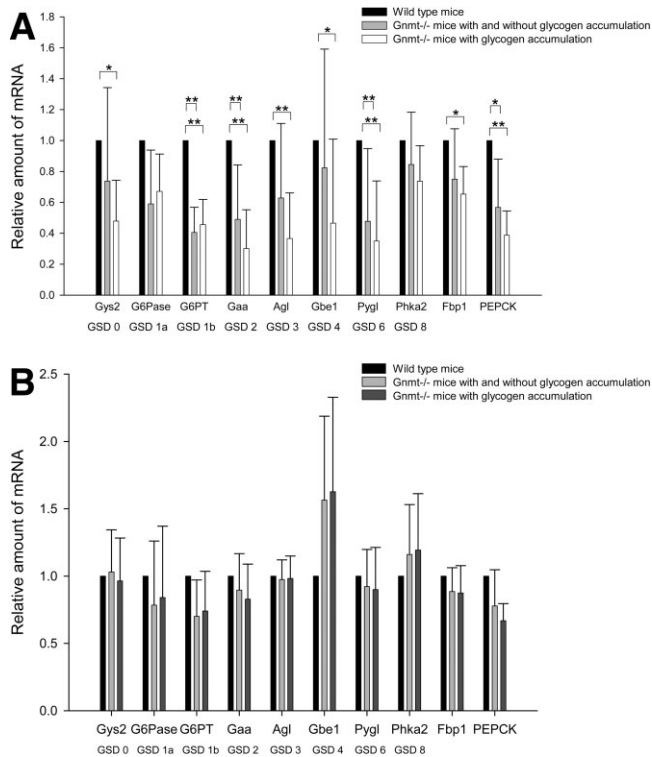


Fig. 7. Real-time polymerase chain reaction analysis of the mRNA expression levels of genes linked with various types of GSDs. The expression profiles of mRNA were normalized to the wild-type mice. (A) Mice at 11 weeks of age. (B) Mice at 9 months of age. **P* < 0.05 and ***P* < 0.01. *Ag1* indicates amylo-1,6-glucosidase; *Fbp1*, fructose 1,6-bisphosphatase; *G6Pase*, glucose-6-phosphatase; *G6PT*, glucose-6-phosphate transporter; *Gaa*, alpha-glucosidase; *Gbe1*, branching enzyme 1; *Gnm1*, glycine N-methyltransferase; GSD, glycogen storage disease; *Gys2*, glycogen synthase 2; mRNA, messenger RNA; *PEPCK*, phosphoenolpyruvate carboxykinase; *Phka2*, phosphorylase kinase alpha 2; and *Pygl*, glycogen phosphorylase.

Gnmt^{-/-} mice was 71-fold higher than that in the wild-type mice; the SAH concentration was the same in the two mouse types (Table 2). Previously, Luka et al.¹⁵ established a *Gnmt*^{-/-} mouse model and found that compared with the wild-type mice, the *Gnmt*^{-/-} mice had a 35-fold higher level of hepatic SAM and a significantly lower level of SAH. In their report, they did not mention the age, gender, or number of the mice that they used for the analysis. Therefore, it is difficult to compare the two models because of the limited information. However, we analyzed the hepatic SAH levels of 9-month-old mice (3 in each group) and found no significant differences between *Gnmt*^{-/-} and wild-type mice (data not shown). In a previous report describing patients with congenital *GNMT* deficiencies, their hepatic SAM levels were 22–40 times higher than the reference value, and the SAH levels remained constant.⁹ In this study, the SAM/SAH ratios were 42 and 67 for male and female *Gnmt*^{-/-} mice, respectively, at 11 weeks of age, and these ratios are compatible with that noted in a 5-year-old boy with a congenital *GNMT* deficiency.⁹ Hypermethioninemia has previously been reported in patients with congenital *GNMT* deficiencies, with serum levels of homocysteine remaining unchanged.^{8,9} This is similar to what we observed in our *Gnmt*^{-/-} mice (Table 2). Therefore, we suggest that our *Gnmt*^{-/-} mouse model is useful for the study of the pathogenesis of congenital *GNMT* deficiencies.

In this study, we found that the mean hepatic concentration of SAM in *Gnmt*^{+/-} mice was about one-third of that in wild-type mice, and the SAM/SAH ratio was reduced from 0.69 to 0.23 (Table 2). This suggests an overcompensation mechanism in hepatocytes that reacts to a reduced *GNMT* level. SAM is an essential metabolite in all cells. It has been proposed that SAM acts as an intracellular control switch that regulates essential hepatic functions such as regeneration, differentiation, and the sensitivity of this organ to injury.¹⁶ It has been reported that in methionine adenosyltransferase 1A (*MAT1A*)^{-/-} mice, the hepatic SAM and glutathione levels decrease, and the mice develop steatohepatitis and hepatomegaly and are susceptible to injury.¹⁷ In this study, the *Gnmt*^{-/-} mice had an extremely high level of SAM, and they developed hepatitis and hepatomegaly. Therefore, the hepatic SAM level needs to be maintained within a certain range, and a deficiency or excess can lead to an abnormality.

We used real-time PCR to analyze the expression levels of genes involved in the one-carbon metabolism pathway. Our results showed that the mRNA of *Ahcy*, *Mthfr*, and *Ftcd* was down-regulated significantly in both male and female *Gnmt*^{-/-} mice (Fig. 3). As shown in Fig. 8A,

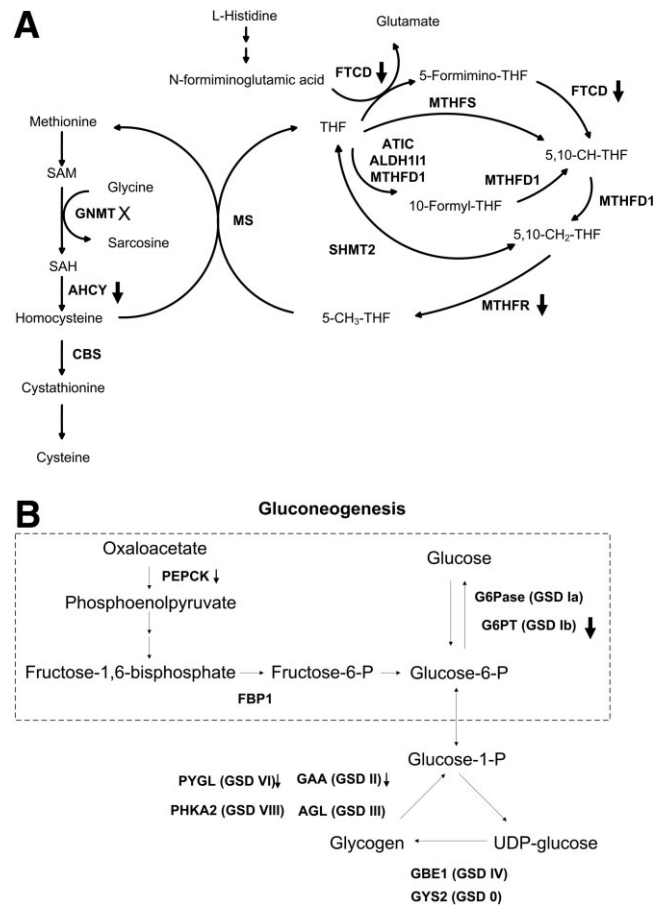


Fig. 8. Effect of a *Gnmt* deficiency on the one-carbon metabolism and glycogen metabolism pathways. (A) Role played by *Gnmt* in the one-carbon metabolism pathway. The results from a real-time PCR analysis show that in comparison with the wild-type mice, the mRNAs of the *Ahcy*, *Mthfr*, and *Ftcd* genes were significantly down-regulated in both male and female *Gnmt*^{-/-} mice. (B) Glycogen metabolism and gluconeogenesis pathway. The results from a real-time PCR analysis show that in comparison with the wild-type mice, the mRNAs of the *G6PT*, *Gaa*, *Pygl*, and *PEPCK* genes were significantly down-regulated in all *Gnmt*^{-/-} and accumulated-glycogen *Gnmt*^{-/-} mice. AGL indicates amylo-1,6-glucosidase; AHCY, S-adenosylhomocysteine hydrolase; ALDH111, aldehyde dehydrogenase 1 family member L1; ATIC, 5-aminoimidazole-4-carboxamide ribonucleotide formyltransferase/IMP cyclohydrolase; CBS, cystathionine beta-synthase; FBP1, fructose 1,6-bisphosphatase; FTCD, formiminotransferase cyclodeaminase; G6Pase, glucose-6-phosphatase; G6PT, glucose-6-phosphate transporter; GAA, α -glucosidase; GBE1, branching enzyme 1; GNMT, glycine N-methyltransferase; GYS2, glycogen synthase 2; mRNA, messenger RNA; MS, methionine synthase; MTHFD1, methylenetetrahydrofolate dehydrogenase (oxidized nicotinamide adenine dinucleotide phosphate-dependent), methylenetetrahydrofolate cyclohydrolase, formyltetrahydrofolate synthase; MTHFR, 5,10-methylenetetrahydrofolate reductase; MTHFS, 5,10-methylenetetrahydrofolate synthetase; PCR, polymerase chain reaction; PEPCK, phosphoenolpyruvate carboxykinase; PHKA2, phosphorylase kinase alpha 2; PYGL, glycogen phosphorylase; and SHMT2, serine hydroxymethyl transferase 2.

Ahcy catalyzes the hydrolytic process of SAH to homocysteine. Homocysteine removal is essential because the equilibrium of the *Ahcy* catalytic reaction strongly favors SAH formation. Under normal conditions, the homocys-

teine turnover rate is sufficient for favoring SAH hydrolysis; this is an important point because SAH is a potent inhibitor of most methyltransferases.^{18,19} AHCY enzyme activity inhibition in rat hepatocytes results in the intracellular accumulation of SAH and the inhibition of SAM-dependent methylation.²⁰ Because AHCY is thought to play a pivotal role in transmethylation reaction control via the regulation of intracellular homocysteine and SAH levels, *Ahcy* down-regulation may play an important role in maintaining the SAH level in the livers of *Gnmt*^{-/-} mice.

MTHFR catalyzes the conversion of 5,10-methyltetrahydrofolate to 5-methyltetrahydrofolate (Fig. 8A).²¹ According to Wagner et al.,²² 5-methyltetrahydrofolate inhibits GNMT enzyme activity. Jencks et al.²³ found that SAM inhibits MTHFR, thereby reducing the supply of methyl groups originating from the one-carbon pool. Accordingly, *Mthfr* down-regulation in *Gnmt*^{-/-} mice may result from the absence of GNMT activity and the accumulation of SAM.

The intermediate metabolism enzyme FTCD links histidine catabolism with folate metabolism. FTCD also catalyzes the folate-dependent degradation of N-formiminoglutamic acid to form 5,10-methylenetetrahydrofolate, glutamate, and ammonia. These reactions are the final 2 steps in the pathway responsible for L-histidine degradation (Fig. 8A).²⁴ Our study is the first demonstration that GNMT can regulate *Ftcd* gene expression. Further studies are needed to determine the underlying mechanism.

Clinically, the Italian girl and her brother with a congenital *GNMT* deficiency had hepatomegaly at the ages of 4.7 and 9.7 years, respectively. However, the Gypsy boy with a *GNMT* deficiency did not have hepatomegaly at the age of 5 years.^{8,9} The ALT and AST values for these 3 patients were also higher than the reference values.^{8,9} We observed hepatomegaly in 4-week-old female *Gnmt*^{-/-} mice but not in male *Gnmt*^{-/-} mice (Fig. 4A). In addition, the mean serum level of ALT in female *Gnmt*^{-/-} mice was significantly higher than that in the wild-type mice ($P < 0.05$); the difference in the serum ALT levels between male *Gnmt*^{-/-} and wild-type mice was not statistically significant (Fig. 4B). This suggests that the absence of GNMT in the liver may induce liver cell damage and that the effects start earlier in the female mice.

Pathological examinations revealed degenerative changes and perinuclear vacuoles in the intermediate zones of female *Gnmt*^{-/-} mouse livers (Fig. 5H,L). Focal necrosis and sinusoid congestion were observed in male *Gnmt*^{-/-} mouse livers (Fig. 5G,K). In addition, PAS staining demonstrated that a higher percentage of female *Gnmt*^{-/-} mice (71.4%) than male *Gnmt*^{-/-}

mice (42.9%) had abnormal glycogen accumulations. All *Gnmt*^{-/-} mice had been fasted for 8 hours before being sacrificed. Previously, Aida et al.⁷ reported that in mouse livers, *Gnmt* expression is much lower in male mice than in female mice and that this expression is regulated by a growth hormone.⁷ We will continue to confirm the diverse responses of liver pathology between male and female *Gnmt*^{-/-} mice.

GSDs, characterized by abnormal inherited glycogen metabolism in the liver, muscle, and brain, are divided into types 0 to X.²⁵ We compared the mRNA levels of a panel of genes responsible for various types of GSDs in wild-type and *Gnmt*^{-/-} mice. Our results showed that the mRNA levels of *G6PT*, *Gaa*, and *Pygl* were significantly lower in the *Gnmt*^{-/-} mice in general and in those with abnormal glycogen accumulations (Figs. 7A and 8B). The down-regulation of G6PT results in a glucose 6-phosphate accumulation that inactivates PYGL.²⁶ Little is known about the interaction between G6PT and GAA. Raben et al.²⁷ generated *Gaa*^{-/-} mice that started to accumulate glycogen in cardiac and skeletal muscle lysosomes by 3 weeks of age, and this was followed by a progressive increase. At 8-9 months of age, these mice developed obvious signs of muscle deterioration and had waddling gaits.²⁷ Neither abnormal glycogen accumulation in the heart and kidneys nor muscle wasting was observed in *Gnmt*^{-/-} mice. We speculate that *G6PT* down-regulation is responsible for the GSD phenotype that we observed in our *Gnmt*^{-/-} mice.

Patients with *G6PT* deficiencies (GSD Ib) suffer from retarded growth, hypoglycemia, hepatomegaly, nephromegaly, hyperlipidemia, hyperuricemia, lactic acidemia, neutropenia, and myeloid dysfunction.²⁸ The phenotypes of the *G6PT*^{-/-} mouse model developed and mimicked those of GSD Ib patients.²⁹ We found that the *Gnmt*^{-/-} and *G6PT*^{-/-} mice shared the following characteristics: hypoglycemia, hepatomegaly, increased cholesterol, glycogen accumulation, and neutropenia, whereas growth retardation, nephromegaly, hyperuricemia, and increased triglyceride levels were not observed in the *Gnmt*^{-/-} mice. With respect to the rate-limiting enzymes involved in the gluconeogenesis pathway (FBP1 and PEPCK), results from a real-time PCR analysis demonstrated that both genes were down-regulated in the *Gnmt*^{-/-} mice with abnormal glycogen accumulations (Fig. 7A). Because of the down-regulation of both *Fbp1* and *PEPCK*, the serum glucose levels of our *Gnmt*^{-/-} mice were significantly lower than those of the wild-type mice.

Previously, Schalinske's group³⁰⁻³² conducted a series of experiments and showed that rat hepatic GNMT activity can be up-regulated by vitamin A, glucocorticoid, and streptozotocin-induced diabetes. In addition, the

treatment of streptozotocin-induced diabetic rats with insulin prevented the induction of GNMT.³³ This suggests that GNMT may play a role in the regulation of gluconeogenesis and glycolysis pathways. In this study, we strengthen this idea by the observation of hypoglycemia and glycogen accumulation in the *Gnmt*^{-/-} mice.

Glycogen retention upon fasting is one of the most important markers of a preneoplastic lesion in the liver.³⁴ In a rat liver tumor model, both clear and eosinophilic cells form multiple foci during the preneoplastic stages of hepatocarcinogenesis.³⁵ The accumulation of glycogen in neoplastic nodules suggests that they originate from foci that store excess glycogen³⁵; patients suffering from type I GSD frequently develop hepatic tumors.³⁶ We previously reported that the expression of GNMT is down-regulated in hepatocellular carcinoma.^{3,4} A genetic epidemiological study has identified *GNMT* as a tumor susceptibility gene for liver cancer⁵; we therefore hypothesize that GNMT down-regulation is an early event during the initiation stage of hepatocarcinogenesis. Interactions between GNMT and environmental carcinogens will be determined in the near future with *Gnmt*^{-/-} mice challenged with various carcinogens.

In summary, hepatomegaly, hypermethioninemia, and significantly higher levels of serum ALT and hepatic SAM were observed in our *Gnmt*^{-/-} mice. The phenotypes mimic those of patients suffering from *GNMT* deficiencies. In addition, hypoglycemia, increased serum cholesterol, and significantly lower numbers of white blood cells, neutrophils, and monocytes were observed in the *Gnmt*^{-/-} mice. The phenotypes share several characteristics with patients with congenital *G6PT* deficiencies. We suggest that this animal model is useful for studies of the pathogenesis of congenital *GNMT* deficiencies and the role of GNMT in glycogen metabolism and in liver tumorigenesis.

Acknowledgment: We thank Dr. Chung-Yung Chen from the Genomic Center of National Yang-Ming University for the sequencing of our phage clones; Dr. Teh-Ying Chou, and Dr. Ting-Yao Chen for their helpful discussions on pathological examinations of liver specimens; Dr. John T. Kung from the genome-wide mutant mouse animal model core facility of the National Research Program on Genomic Medicine; Mr. Yi-Cheng Wang from the Department of Food Science and Biotechnology at National Chung Hsing University for the determination of SAM, SAH, and homocysteine; and members of the Division of Preventive Medicine of the Public Health Institute at National Yang-Ming University for their technical support.

References

1. Yeo EJ, Wagner C. Tissue distribution of glycine N-methyltransferase, a major folate-binding protein of liver. *Proc Natl Acad Sci U S A* 1994;91:210-214.
2. Kerr SJ. Competing methyltransferase systems. *J Biol Chem* 1972;247:4248-4252.
3. Chen YM, Shiu JY, Tzeng SJ, Shih LS, Chen YJ, Lui WY, et al. Characterization of glycine-N-methyltransferase-gene expression in human hepatocellular carcinoma. *Int J Cancer* 1998;75:787-793.
4. Liu HH, Chen KH, Shih YP, Lui WY, Wong FH, Chen YM. Characterization of reduced expression of glycine N-methyltransferase in cancerous hepatic tissues using two newly developed monoclonal antibodies. *J Biomed Sci* 2003;10:87-97.
5. Tseng TL, Shih YP, Huang YC, Wang CK, Chen PH, Chang JG, et al. Genotypic and phenotypic characterization of a putative tumor susceptibility gene, GNMT, in liver cancer. *Cancer Res* 2003;63:647-654.
6. Chen SY, Lin JR, Darbha R, Lin P, Liu TY, Chen YM. Glycine N-methyltransferase tumor susceptibility gene in the benzo(a)pyrene-detoxification pathway. *Cancer Res* 2004;64:3617-3623.
7. Aida K, Tawata M, Negishi M, Onaya T. Mouse glycine N-methyltransferase is sexually dimorphic and regulated by growth hormone. *Horm Metab Res* 1997;29:646-649.
8. Mudd SH, Cerone R, Schiaffino MC, Fantasia AR, Minniti G, Caruso U, et al. Glycine N-methyltransferase deficiency: a novel inborn error causing persistent isolated hypermethioninaemia. *J Inher Metab Dis* 2001;24:448-464.
9. Augoustides-Savvopoulou P, Luka Z, Karyda S, Stabler SP, Allen RH, Patsiaoura K, et al. Glycine N-methyltransferase deficiency: a new patient with a novel mutation. *J Inher Metab Dis* 2003;26:745-759.
10. Sambrook PN, Champion GD, Browne CD, Cairns D, Cohen ML, Day RO, et al. Corticosteroid injection for osteoarthritis of the knee: peripatellar compared to intra-articular route. *Clin Exp Rheumatol* 1989;7:609-613.
11. Anderson S. Shotgun DNA sequencing using cloned DNase I-generated fragments. *Nucleic Acids Res* 1981;9:3015-3027.
12. Dierlamm J, Wlodarska I, Michaux L, La SR, Zeller W, Mecucci C, et al. Successful use of the same slide for consecutive fluorescence in situ hybridization experiments. *Genes Chromosomes Cancer* 1996;16:261-264.
13. Lee CM, Chen SY, Lee YC, Huang CY, Chen YM. Benzo[a]pyrene and glycine N-methyltransferase interactions: gene expression profiles of the liver detoxification pathway. *Toxicol Appl Pharmacol* 2006;214:126-135.
14. Araki A, Sako Y. Determination of free and total homocysteine in human plasma by high-performance liquid chromatography with fluorescence detection. *J Chromatogr* 1987;422:43-52.
15. Luka Z, Capdevila A, Mato JM, Wagner C. A glycine N-methyltransferase knockout mouse model for humans with deficiency of this enzyme. *Transgenic Res* 2006;15:393-397.
16. Mato JM, Corrales FJ, Lu SC, Avila MA. S-Adenosylmethionine: a control switch that regulates liver function. *FASEB J* 2002;16:15-26.
17. Lu SC, Tsukamoto H, Mato JM. Role of abnormal methionine metabolism in alcoholic liver injury. *Alcohol* 2002;27:155-162.
18. James SJ, Melnyk S, Pogribna M, Pogribny IP, Caudill MA. Elevation in S-adenosylhomocysteine and DNA hypomethylation: potential epigenetic mechanism for homocysteine-related pathology. *J Nutr* 2002;132:S2361-S2366.
19. Zhu BT. On the mechanism of homocysteine pathophysiology and pathogenesis: a unifying hypothesis. *Histol Histopathol* 2002;17:1283-1291.
20. Schanche JS, Schanche T, Ueland PM, Montgomery JA. Inactivation and reactivation of intracellular S-adenosylhomocysteinase in the presence of nucleoside analogues in rat hepatocytes. *Cancer Res* 1984;44:4297-4302.
21. Schwahn BC, Chen Z, Laryea MD, Wendel U, Lussier-Cacan S, Genest J Jr, et al. Homocysteine-betaine interactions in a murine model of 5,10-methylenetetrahydrofolate reductase deficiency. *FASEB J* 2003;17:512-514.
22. Wagner C, Briggs WT, Cook RJ. Inhibition of glycine N-methyltransferase activity by folate derivatives: implications for regulation of methyl group metabolism. *Biochem Biophys Res Commun* 1985;127:746-752.
23. Jencks DA, Mathews RG. Allosteric inhibition of methylenetetrahydrofolate reductase by adenosylmethionine. Effects of adenosylmethionine and NADPH on the equilibrium between active and inactive forms of the enzyme and on the kinetics of approach to equilibrium. *J Biol Chem* 1987;262:2485-2493.

24. Solans A, Estivill X, de la Luna S. Cloning and characterization of human FTCD on 21q22.3, a candidate gene for glutamate formiminotransferase deficiency. *Cytogenet Cell Genet* 2000;88:43-49.
25. Shin YS. Glycogen storage disease: clinical, biochemical, and molecular heterogeneity. *Semin Pediatr Neurol* 2006;13:115-120.
26. Voet D, Voet JG. Glycogen metabolism. In: *Biochemistry*. 3rd ed. Hoboken, NJ: John Wiley & Sons; 2004:626-656.
27. Raben N, Nagaraju K, Lee E, Kessler P, Byrne B, Lee L, et al. Targeted disruption of the acid alpha-glucosidase gene in mice causes an illness with critical features of both infantile and adult human glycogen storage disease type II. *J Biol Chem* 1998;273:19086-19092.
28. Chou JY, Matern D, Mansfield BC, Chen YT. Type I glycogen storage diseases: disorders of the glucose-6-phosphatase complex. *Curr Mol Med* 2002;2:121-143.
29. Chen LY, Shieh JJ, Lin B, Pan CJ, Gao JL, Murphy PM, et al. Impaired glucose homeostasis, neutrophil trafficking and function in mice lacking the glucose-6-phosphate transporter. *Hum Mol Genet* 2003;12:2547-2558.
30. Rowling MJ, McMullen MH, Schlinske KL. Vitamin A and its derivatives induce hepatic glycine N-methyltransferase and hypomethylation of DNA in rats. *J Nutr* 2002;132:365-369.
31. Rowling MJ, Schalinske KL. Retinoic acid and glucocorticoid treatment induce hepatic glycine N-methyltransferase and lower plasma homocysteine concentrations in rats and rat hepatoma cells. *J Nutr* 2003;133:3392-3398.
32. Nieman KM, Rowling MJ, Garrow TA, Schalinske KL. Modulation of methyl group metabolism by streptozotocin-induced diabetes and all-trans-retinoic acid. *J Biol Chem* 2004;279:45708-45712.
33. Nieman KM, Schelinske KL. Modulation of methyl group and homocysteine methylation metabolism by insulin treatment in diabetes rats. *FASEB J* 2006;20:A607.
34. Bannasch P, Hacker HJ, Klimek F, Mayer D. Hepatocellular glycogenesis and related pattern of enzymatic changes during hepatocarcinogenesis. *Adv Enzyme Regul* 1984;22:97-121.
35. Hacker HJ, Moore MA, Mayer D, Bannasch P. Correlative histochemistry of some enzymes of carbohydrate metabolism in preneoplastic and neoplastic lesions in the rat liver. *Carcinogenesis* 1982;3:1265-1272.
36. Limmer J, Fleig WE, Leupold D, Bittner R, Ditschuneit H, Beger HG. Hepatocellular carcinoma in type I glycogen storage disease. *HEPATOLOGY* 1988;8:531-537.